7-10-2009

R992C (p.R1192C) Substitution in collagen II alters the structure of mutant molecules and induces the unfolded protein response.

Hye Jin Chung
Thomas Jefferson University

Deborah A. Jensen
Thomas Jefferson University

Katarzyna Gawron
Thomas Jefferson University

Andrzej Steplewski
Thomas Jefferson University

Andrzej Fertala
Thomas Jefferson University, andrzej.fertala@jefferson.edu

As submitted to: *Journal of Molecular Biology*

and later published as:

Volume 390, Issue 2, 10 July 2009, Pages 306-318

DOI: 10.1016/j.jmb.2009.05.004

R992C (p.R1192C) Substitution in Collagen II Alters the Structure of Mutant Molecules and Induces the Unfolded Protein Response.

Hye Jin Chung[1], Deborah A. Jensen[1], Katarzyna Gawron[1], Andrzej Steplewski[1], and Andrzej Fertala[1]*

[1]Department of Dermatology and Cutaneous Biology, Jefferson Medical College, Thomas Jefferson University, Philadelphia, PA 19107, USA.

[*]Corresponding author: Dr. Andrzej Fertala, Department of Dermatology and Cutaneous Biology, Jefferson Medical College, Thomas Jefferson University, BLSB, Room 424, 233 S. 10th Street, Philadelphia, PA 19107, U.S.A.

Tel: 215-503-0113

Running title: Effects of the R992C substitution in collagen II.

Fax: 215-503-5788

E-mail: andrzej.fertala@jefferson.edu

Running title: Effects of the R992C substitution in collagen II.

Summary

We investigated the molecular bases of spondyloepiphyseal dysplasia (SED) associated with the R992C (p.R1192C) substitution in collagen II. At the protein level we analyzed the structure and integrity of mutant molecules, and at the cellular level we specifically studied the effects of the presence of the R992C collagen II on the biological processes taking place in host cells. Our studies demonstrated that mutant collagen II molecules were characterized by altered electrophoretic mobility, relatively low thermostability, the presence of atypical disulfide bonds, and slow rates of secretion into the extracellular space. Analyses of cellular responses to the presence of the mutant molecules showed that excessive accumulation of thermolabile collagen II was associated with the activation of an "unfolded protein response" and an increase in apoptosis of host cells. Collectively, these data suggest that molecular mechanisms of SED may be driven not only by structural changes in the architecture of extracellular collagenous matrices, but also by intracellular processes activated by the presence of mutant collagen II molecules.

Keywords: collagen II mutations; unfolded protein response; ER stress; extracellular matrix; apoptosis

Introduction

Collagen II, a main structural protein of cartilaginous tissues, is first synthesized as procollagen characterized by the presence of an extended triple-helical domain flanked by the globular N-terminal and C-terminal propeptides [1]. Biosynthesis of procollagen molecules is a complex process that involves posttranslational modifications of the nascent pro-α chains. These modifications include hydroxylation of proline residues and lysine residues by prolyl-4 hydroxylase (P4H) and lysyl hydroxylase (LH), respectively. Moreover, the posttranslational modifications and subsequent formation of the triple-helical structure are controlled by a group of endoplasmic reticulum (ER)-resident protein chaperones that includes heat shock protein 47 (HSP47), immunoglobulin-binding protein (BiP), and protein disulfide isomerase (PDI), an enzyme that also acts as the β-subunit of the αα/ββ tetramer that constitutes functional P4H [2,3,4,5]. In addition, by binding to the individual pro-α1(II) chains and preventing their premature association, P4H may also act as a chaperone during biosynthesis of procollagen molecules [6]. Following biosynthesis of individual pro-α1(II) chains, their posttranslational modifications, and folding into triple-helical structure, procollagen molecules are released from the ER and directed toward secretory pathways.

A critical triple-helical domain of collagen II consists of α1(II) chains formed by about 330 G-X-Y triplets in which the "X" position is frequently occupied by a proline residue and the "Y" position by a hydroxyproline residue. The importance of correct conformation of the triple-helical region for the proper structure and function of skeletal tissues is clearly evidenced by a number of aberrations of these tissues caused by mutations in *COL2A1* (**OMIM# 120140**). In particular, single amino acid substitutions in collagen II are responsible for a broad spectrum of

chondrodysplasia phenotypes, generally described as spondyloepiphyseal dysplasia (SED), whose main feature is abnormalities of skeletal development [1,7,8,9,10,11,12,13]. The most frequent amino acid substitutions in collagen II occur at the "G" position of the G-X-Y triplets but substitutions in the "Y" positions were also described. For instance, a G853E (p.G1053E) substitution was found in a patient with a lethal form of SED, whereas cysteine substitutions for arginine residues were found in the "Y" positions 75 (p.R275C), 519 (p.R719C), and 789 (p.R989C) in patients with a mild form of SED, a mild form of osteoarthritis, and a severe form of congenital SED, respectively [9,13,14,15]. In addition to mutations found in the "G" and "Y" positions, relatively rare mutations in the "X" positions of the G-X-Y triplets were also reported in patients with Stickler syndrome, a disease characterized by myopia, cataracts, retinal detachment, hearing loss, and mild SED [13,16,17].

The molecular bases of tissue-level aberrations in patients with mutations in *COL2A1* are not fully understood. It has been suggested that a key problem caused by amino acid substitutions in collagen II is that the mutant collagens cannot fulfill their structural functions. Studies demonstrated that a decrease in the overall content of collagen II and its inability to assemble into correct fibrils are the main factors causing such alterations of structural functions [13,18,19,20,21]. In addition to affecting extracellular functions, it has been suggested that some mutations in collagen II cause excessive intracellular accumulation of misfolded mutant molecules and that such accumulation can lead to apoptosis of cells harboring mutant molecules [22,23].

Here, we studied the molecular and the cellular-level consequences of the R992C (p.R1192C) substitution in the "X" position of a G-X-Y triplet of collagen II. This mutation (p.R1147C) was originally described in mice, referred to as spondyloepiphyseal dysplasia

congenita or *sedc* mice in which skeletal abnormalities were similar to those seen in SED patients [24]. Employing a system for expressing recombinant collagen II, we demonstrated that the R992C collagen II is characterized by aberrant electrophoretic mobility, relatively low thermostability, and the presence of intramolecular disulfide bonds. Moreover, we showed that the expression of the R992C collagen II is associated with ER stress and increased apoptosis of cells harboring this collagen mutant.

Results presented here contribute to understanding the molecular basis of mutation-triggered pathological changes seen at the level of skeletal tissues and suggest that mutations in collagen II that interfere with correct folding of the collagen triple helix are likely to act not only by disturbing the extracellular collagenous framework but also by altering intracellular processes.

Results

Analysis of R992C mutant.

To analyze mutant collagen molecules, we produced the green fluorescence protein (GFP)-tagged wild type procollagen II (WT Pro-GFP) and R992C procollagen II (R992C Pro-GFP) in HT-1080 cells, as described [25]. Electrophoresis of intact GFP-tagged procollagen molecules carried out in 6% polyacrylamide gels demonstrated that the electrophoretic mobility of the R992C Pro-GFP was slower than that of the WT Pro-GFP (Fig. 1). Similar differences in the electrophoretic mobilities were seen in pepsin-treated variants in which non-triple-helical propeptides were enzymatically degraded (Fig. 1). In addition to the intact α1(II) mutant chains, their degraded forms were inconsistently seen in different protein preparations (Fig. 1). The treatment of collagen II variants with glycosidases demonstrated that slower migration of the

R992C mutant was not caused by overglycosylation of mutant collagen α1(II) chains. In this experiment only a minor shift in the migration of glycosidase-treated wild type and mutant collagens was observed (Fig. 1). Such a minor shift in migration indicates relatively small levels of glycosylation of the α1(II) chains, an observation consistent with our previous report [25]. Since no change in the electrophoretic migration of the R992C collagen treated with various denaturing agents was observed, we excluded atypical aggregation as the reason for the slow electrophoretic mobility of this protein (data not shown). Analysis of collagen chains separated in non-reducing conditions demonstrated that about 6% of α1(II) chains were covalently linked by disulfide bonds (Fig. 1). The identity of disulfide-linked chains was confirmed by separating α1(II) monomers and dimers in nonreducing conditions followed by electrophoresis of separated chains in the reducing conditions (Fig. 2).

Analyses of thermostability of the R992C mutant.

Brief protease digestion of pepsin-treated collagen II demonstrated that the thermostability of the R992C mutant was lower than that of the control (Fig. 3). Specifically, we measured the temperatures at which the triple helical structure of analyzed collagens was preserved in 75% (Tm_{75}), 50% (Tm_{50}), and 25% (Tm_{25}) of maximum. We determined that Tm_{75}, Tm_{50}, and Tm_{25} for the R992C were 36.5°C, 39.9°C, and 42.0°C, respectively. Corresponding Tm_{75}, Tm_{50}, and Tm_{25} values for the WT collagen II were 40.0°C, 41.2°C, and 42.2°C, respectively. In contrast to the wild type collagen II, protease digestion of the R992 mutant at about 36°C resulted in the generation of intermediate stable products (Fig. 3).

Computer modeling of the R992C mutation site.

To study the structural basis of formation of disulfide bonds we performed computer modeling of the region encompassing the C992 mutation site (Fig. 4). In this study the modeled collagen fragment consisted of three mutant α1(II) chains. Such a model provides good representation of the homotrimeric R992C collagen II produced in HT-1080 cells and in homozygotic mutant mice, in which the R992C mutation was associated with severe SED [24]. Analysis of the model revealed that sulfhydryl groups of cysteine residues present in two α1(II) chains were spatially oriented in a way that enables formation of the disulfide bonds. Moreover, the model revealed that the sulfhydryl group of the free cysteine residue was exposed on the surface of a molecule, thereby rendering it available for formation of intermolecular disulfide bonds. In addition, analysis of molecular surfaces demonstrated that the cysteine for arginine substitution decreased the electrostatic potential (EP) of a region encompassing the mutation site. Specifically, the EP values (expressed in kcal/mol.e) for the region with a molecular surface area of about 1000 $Å^2$ and encompassing the R992 residue ranged from 117.7 to 233.4. In contrast, the corresponding EP values for the analogous region encompassing the C992 site ranged from 28.2 to 127.2.

Unconditional and Tet-regulated expression of procollagen II variants in SW-1353 cells.

We generated a system for unconditional and tetracycline (Tet)-regulated expression of procollagen II variants. Procollagen II variants expressed unconditionally were denoted as "Pro-GFP" whereas those expressed in the Tet-regulated fashion, as "Pro-GFP^{Tet}". To account for possible differences in measured parameters, due to clonal variations in expression of the R992C mutant, two independent R992C Pro-GFP and two R992C Pro-GFP^{Tet} clones were analyzed in

more detail. The biosynthesis of procollagen II variants expressed in SW-1353 cells was characterized by Western blot and RT-PCR assays. As indicated in Fig. 5, procollagen II was efficiently expressed in both systems. Moreover, in the Tet-regulated system expression of procollagen II was efficiently expressed only in the presence of doxycycline (Dox). In one of the R992C Pro-GFP^{Tet} clones (clone #2) there was a detectable baseline-level expression of the R992C Pro-GFP^{Tet} mRNA. Such a baseline expression is expected due to nonspecific activation of a Tet-regulated cytomegalovirus (CMV) promoter [26]. As indicated in Fig. 5 expression of procollagen variants was comparable at both the mRNA and protein levels.

In addition to analysis of the intracellular pool of the R992C collagen II, we also studied kinetics of secretion of this mutant in comparison to WT control (Fig. 6). Assays of Pro-GFP from two different clones harboring the R992C collagen II demonstrated that the secretion rate of this mutant, represented by the slope of a fitted curve, was slower in comparison to WT control. In particular, after six hours from the beginning of the experiment the relative amount of the R992 Pro-GFP present in the media was only about 40% of WT Pro-GFP secreted from the same number of cells. In all analyses of the secretion rates, the R^2 values ranged from 0.9 to 1.0, indicating a satisfactory curve fit.

Apoptotic markers in cells expressing R992C mutant.

Cellular apoptosis was assayed by TdT-mediated dUTP nick-end labeling (TUNEL) (Fig. 7) and measurements of the relative content of cleaved poly (ADP-ribose) polymerase (PARP) (Fig. 8). In the TUNEL assays the apoptotic index was defined as the percentage of the TUNEL-positive cells out of the total number of 4',6-diamidino-2-phenylindole (DAPI)-stained nuclei. The R992C Pro-GFP variant had a higher apoptotic index, corresponding to 4.2%±0.5%, than

the WT Pro-GFP with an apoptotic index of 2.2%±0.2%. Statistical analysis with the Student's *t* test revealed that the difference between mean values for two groups was statistically significant (*P=0.0042*) (Fig. 7). To confirm that DNA fragmentation was a direct result of the presence of the R992C mutant, we employed cells conditionally expressing the R992C Pro-GFP^{Tet} variant. In the Tet-ON condition, in the presence of the R992C mutant, the apoptotic index (4.8%±0.4%) was significantly higher (*P=0.0037*) than in cells cultured in the Tet-OFF condition (3.2%±0.3%). In contrast, regardless of Tet-ON or Tet-OFF conditions, apoptotic indexes for cells engineered to express the WT Pro-GFP^{Tet} did not show any significant difference (*P=0.4744*).

Multiple analyses of two different clones expressing the R992C Pro-GFP variant and two different clones expressing the R992C Pro-GFP^{Tet} variant revealed that the relative amount of cleaved PARP increased in cells harboring the R992C mutant (Fig. 8). Specifically, in the cells harboring the R992C Pro-GFP variant, the relative amount of cleaved PARP increased 2.2-fold in comparison to control (*P=0.009*). Moreover, in comparison to control, the relative amount of cleaved PARP after induction with Dox increased 2.8-fold (*P=0.004*). In contrast, in cells expressing the WT Pro-GFP adding Dox did not increase the relative amount of cleaved PARP (*P=0.756*).

Measurements of selected indicators of ER stress.

We employed Western blot assays to analyze selected indicators of ER stress. As shown in Fig. 9, the relative amount of PDI in cells expressing the R992C Pro-GFP variants increased 2.3-fold in comparison to control (*P=0.032*). Analysis of Pro-GFP^{Tet} system also revealed that the Dox-induced R992C Pro-GFP^{Tet} variant increased the relative amount of PDI 1.9-fold

(*P=0.0004*), while Dox-induced WT Pro-GFP^{Tet} did not show any significant difference (*P=0.839*). Western blotting of BiP also revealed a similar trend, although the 2.4-fold increase in the relative amount of BiP in the R992C Pro-GFP variant was not statistically significant (*P=0.215*) (Fig. 9). However, the 3.2-fold increase in the BiP content in Dox-stimulated cells expressing the R992C Pro-GFP^{Tet} was statistically significant (*P=0.003*).

Analysis of LH and P4H.

We studied whether the presence of the mutant α1(II) chains could be associated with increased expression of LH and P4H. Our analyses revealed that the relative amounts of LH (Fig. 9) and the α-subunit of P4H (P4Hα; not shown) in cells expressing the R992C mutant were similar to that of control.

In situ colocalization of BiP, PDI, and P4H with the R992C Pro-GFP.

To examine the potential interaction of selected chaperones with mutant collagen II *in situ,* we employed fluorescence microscopy to analyze colocalization of BiP and PDI with WT Pro-GFP and R992C Pro-GFP variants (Fig. 10). Considering that PDI functions not only independently as protein disulfide-isomerase but also acts as the β-subunit of P4H, we studied the colocalization of the α-subunit of this enzyme with Pro-GFP variants. These studies were critical for determining whether in response to the presence of mutant collagen II, PDI interacted with Pro-GFP variants independently or as a member of the αα/ββ P4H complex. To describe colocalization of BiP/Pro-GFP, PDI/Pro-GFP and P4Hα/Pro-GFP we used the overlap coefficient (*R*), a value that ranges from 0 and 1 and is not sensitive to variations in pixel intensities. We demonstrated that in comparison to the cells expressing WT Pro-GFP

(*R*=0.61±0.015; N=66) the overlap coefficient for PDI/Pro-GFP colocalization was higher in cells expressing the R992C Pro-GFP (*R*=0.72±0.010; N=69). Moreover, we analyzed BiP/Pro-GFP colocalization, and our study determined that in comparison to cells expressing WT Pro-GFP (*R*=0.28±0.012; N=40) the value for the overlap coefficient decreased in cells expressing R992C Pro-GFP (*R*=0.14±0.009; N=43). Statistical analysis determined that the differences in the *R* values for PDI/Pro-GFP and BiP/Pro-GFP colocalization were statistically significant with *P<0.0001*. In addition, we determined that, in comparison to PDI and BiP, the overlap coefficient for P4Hα/Pro-GFP colocalization was relatively low for cells expressing WT Pro-GFP (*R*=0.16±0.009; N=39), and it did not significantly change (*P=0.8*) in cells expressing the R992C Pro-GFP variant (*R*=0.15±0.008; N=30).

Discussion

Contrary to the mutations in the "G" and "Y" positions, the molecular and cellular-level consequences of the "X" position amino acid substitutions in collagen II have not described. Here, we studied the molecular and cellular effects of the "X" position R992C substitution in collagen II found in mice with pathological skeletal features resembling those of SED [24]. More recently, we presented evidence that in the growth plates of these mutant mice chondrocytes include dilated ER cysternae and the number of cells undergoing apoptosis is higher than in control [23]. The molecular bases of such cellular changes, however, were not determined [23].

In the present study we showed that α1(II) chains of collagen II with the R992C substitution are characterized by relatively slow electrophoretic mobility and the existence of intramolecular

disulfide bonds. Relatively slow electrophoretic mobility of the mutant α1(II) chains was not a result of their excessive glycosylation. Because the electrophoretic mobility of fibrillar collagens does not strictly follow principles that govern migration of globular proteins, it is difficult to fully explain the aberrant behavior of the R992C mutant. We postulate, however, that the delayed electrophoretic mobility of the R992C mutant in the absence of evident chemical overmodifications could be a result of its structural alterations. In support of this notion is the report by Forlino *et al*. where delayed mobility of α2(I) chains harboring G421D substitution in the absence of the overmodifications was attributed to a structural change represented by a kink formed in some mutant collagen I molecules [27]. Moreover, in our own studies on R789C collagen II we observed structural aberrations and determined that the electrophoretic mobility of this mutant was slower than that of wild type collagen II [28].

Consequences of structural aberrations of the R992C collagen molecules include their slow secretion from cells, lower thermostability, and formation of intramolecular disulfide bonds between about 6% of the α1(II) chains. Formation of disulfide bonds in the R75C, R519C, and R789C collagen II mutants isolated from patients' tissues or in corresponding recombinant mutants expressed in HT-1080 cells was also reported [15,19,28,29]. A common characteristic of those mutants is that, unlike in the R992C collagen, the C for R substitutions occur at the "Y" positions of G-X-Y triplets.

Structural aberrations of the R992C collagen II are further illustrated by the formation of stable intermediate products of the digestion of this protein with trypsin and chymotrypsin. In accordance with the concept of micro-unfolding of a collagen triple-helix, it has been suggested that the presence of such intermediate products is evidence for the destabilization of cooperative blocks [30,31]. As suggested by Westerhausen *et al*., certain amino acid substitutions may expose

trypsin/chymotrypsin-sensitive sites at relatively low temperatures, thereby leading to the generation of intermediate collagen fragments of varying sizes [31]. The 1°C-decrease in thermostability (Tm_{50}) in the R992C mutant is relatively small in comparison to the 5°C-decrease of thermostability in the R789C mutant [28]. It is expected, however, that the change of the triple helix-stabilizing arginine residue to the triple helix-destabilizing cysteine residue is significant for the overall structure and physicochemical characteristics, such as the electrostatic potential, and the stability of the region encompassing the mutation site [32]. In particular, the R992C substitution may interfere with functions of the neighboring C-terminal triple-helix-stabilizing "knot" that is formed by tandem repeats of triple helix-stabilizing G-P-P triplets [33].

In our previous studies on collagen II mutants we observed that, in contrast to thermostable R75C, R519C, and G853E mutants, the thermolabile R789C mutant was associated with apoptosis of host cells. The direct role of this mutant in triggering the apoptotic changes was demonstrated in chondrocytic cells in which the production of the R789C Pro-GFP^{Tet} was induced by Dox. Here, we also employed a Tet-inducible system for expressing the R992C Pro-GFP^{Tet}, and our results indicate that the presence of this mutant is directly responsible for the increase in the number of cells undergoing apoptosis. In comparison to the R789C mutant, however, the relative content of cleaved PARP, an indicator of apoptosis, was significantly lower in cells expressing the R992 Pro-GFP or R992C Pro-GFP^{Tet} variants. A less severe apoptotic response of the chondrocytic cells expressing the exogenous R992C collagen II together with endogenous wild type collagen II could explain the observation that SED-like characteristics of skeletal tissues were only apparent in *sedc* mice expressing the mutant *Col2a1* in a homozygous way [24]. Still, we postulate that the possibility of mild aberrations at molecular and cellular levels in heterozygous *sedc* mice cannot be completely excluded.

Because of the apparent increase in the expression of BiP and PDI in response to the presence of the R992C collagen II, our study suggests activation of the unfolded protein response process in cells expressing this thermolabile mutant. In addition to the increase in the biosynthesis of PDI, we also demonstrated increased *in situ* colocalization of this chaperone with the R992C Pro-GFP. Because PDI not only functions independently but also serves as the β-subunit of the αα/ββ tetramer which constitutes functional P4H, we studied the specificity of the increase in the biosynthesis of PDI and its elevated colocalization with R992C Pro-GFP. Our studies with the anti-P4Hα antibodies determined that, in comparison to cells expressing WT Pro-GFP, the quantity of P4H and its colocalization with R992C Pro-GFP did not change. These observations suggest that, in response to the presence of the R992C mutant, PDI enhances rather its chaperone roles than its P4H-related functions. The increased colocalization of PDI with R992C Pro-GFP may indicate an increase in the PDI/R992C Pro-GFP binding. Such a notion is justified by observations that PDI preferably binds to the nascent procollagen α chains, but it may remain bound even after the α chains fold into a triple-helical structure [2,34]. As demonstrated with certain collagen I mutants, PDI facilitates intracellular retention of aberrant collagen molecules by binding to misfolded α chains. Such PDI-mediated retention of the R992C Pro-GFP is suggested by its slow rate of secretion from the host cells.

In contrast to PDI, *in situ* colocalization of BiP decreased in the cells expressing the R992C mutant. The role of BiP in retention of misfolded protein molecules is less clearly defined and somewhat controversial [3,35]. Based on the studies of collagen I and collagen II mutants, it has been suggested that this molecule interacts with collagen weakly, and it preferably binds to the triple-helical structure of the collagen molecule [3,23].Thus, we propose that the decrease in

colocalization of the R992C Pro-GFP with BiP could be a result of altered triple-helicity of the BiP-binding regions, blocking of the BiP-binding sites by PDI, or both.

Our studies presented here indicate that pathomechanisms responsible for altering skeletal tissues harboring single amino acid substitutions in collagen II include those that function at the intracellular level. In the future, detailed studies of biological processes triggered by the presence of mutant collagen molecules will reveal specific pathways that lead from altered collagen structure to the apoptosis of affected cells. Understanding such pathways will be critical for determining a genotype/phenotype relation in heritable diseases caused by mutations in genes that encode fibrillar collagens.

Materials and Methods

Mutation nomenclature.

The amino acid substitutions are named according to the literature, with amino acid residues numbered from the first glycine of the collagen II triple helix. At their initial text appearances the mutations are also numbered from the ATG start codon following the journal and the Human Genome Variation Society guidelines (www.hgvs.org) and are listed in parentheses (with a “p” included in the mutation name).

Engineering cDNA constructs for unconditional and Tet-regulated expression of GFP-tagged procollagen II variants.

Although the R992C substitution was originally described in mice, to study the consequences of this mutation at the molecular level, we employed a system that utilizes human collagen II. Such an approach is justified because of the high similarity between amino acid sequences of mouse (**NP_112440.1**) and human collagen II (**NP_001835.3**); in the region encompassing the mutation site, this similarity is 100%. A DNA construct for expression of the procollagen II mutant with the R992C substitution was assembled from DNA cassettes which encode specific domains of human procollagen II, as described [21,36,37]. In particular, a DNA construct was created by mutating the –CGA- codon for R992 to the –TGC- codon for C992 (Quick Change mutagenesis kit, Stratagene, Inc.).

For the unconditional expression of the GFP-tagged R992C procollagen II, denoted as R992C "Pro-GFP", a DNA construct was cloned into the pEGFP-N3 vector (Clontech Laboratories, Inc.), as described [22]. In addition, to study the specific biological responses of cells to the presence of the R992C mutant, we employed a conditional expression system in which the expression of GFP-tagged procollagen II variants, denoted as "Pro-GFP^{Tet}", was regulated by a Tet-responsive promoter (Clontech Laboratories, Inc.), as described [23]. The fidelity of all DNA constructs was determined by sequencing.

Analysis of procollagens and collagens variants expressed in HT-1080 cells.

To obtain procollagen II for protein analyses, the WT Pro-GFP and the R992C Pro-GFP variants were expressed in HT-1080 cells (ATCC, CCL-121), as described [25]. These procollagen II variants were isolated from cell culture media and purified by ion exchange chromatography,

as described [25]. Because the R992C procollagen II variant was relatively unstable and over time underwent partial degradation, for analyses of collagen II variants, procollagen secreted to cell culture media was precipitated with ammonium sulfate, as described. Pellets were suspended in 0.5 M acetic acid and then dialyzed against this solvent. Acetic acid-insoluble material was removed by centrifugation, and then proteins were digested for 48 h at 4°Cwith pepsin (Sigma-Aldrich) added to the final concentration of 0.1 mg/ml. Pepsin-resistant collagen was precipitated with 0.7 M NaCl and then collected by centrifugation.

Analysis of intact Pro-GFP and pepsin-processed collagen variants.

Freshly isolated intact procollagen II variants secreted to cell culture media and pepsin-treated collagens were analyzed by electrophoresis. To visualize any potential differences in the electrophoretic mobilities of analyzed proteins, electrophoresis was carried out in 6% polyacrylamide gels and continued until a 50-kDa molecular mass marker had reached the lower edge of polyacrylamide gels. To facilitate specific detection of relatively small amounts of analyzed proteins, intact Pro-GFP variants were transferred to nitrocellulose membranes and visualized by immunostaining with anti-GFP antibody (Santa Cruz Biotechnology, Inc) and secondary anti-mouse IgG conjugated with horseradish peroxidase (HRP, Sigma-Aldrich). Specific bands were visualized by chemiluminescence (UVP, LLC). Similarly, pepsin-treated collagens were detected with anti-collagen II antibody (Millipore). Note that neither antibodies cross-react with proteins secreted from untransfected HT-1080 cells.

Treatment of collagen II with selected glycosidases and denaturing agents.

To determine if delayed electrophoretic migration of the mutant α1(II) chains could be a result of their overglycosylation, we employed neuraminidase, N-glycosidase F, and endo-α-N-acetylgalactosaminidase (New England BioLabs, Inc.) to remove collagen-bound carbohydrates [25]. After treatment with selected enzymes, α1(II) chains were electrophoresed in polyacrylamide gels and the extents of their electrophoretic migrations were evaluated.

To exclude the possibility that the delayed migration of the R992C collagen II could be a result of its aggregation, we treated this mutant with selected agents that promote the dissociation of macromolecular complexes. Specifically, we employed 4 M urea, 4 M guanidinium hydrochloride, 0.5 M acetic acid or 50% dimethyl sulfoxide. Individual samples of wild type and R992C mutant were treated with these compounds for 48 h. Subsequently, electrophoretic migrations of collagen samples were analyzed.

Analysis of disulfide bonds.

The intramolecular disulfide bonds formed between the C992 residues were assayed by electrophoresis. In brief, initially the α-chains of pepsin-treated collagen II were separated in 7.5% polyacrylamide gels under non-reducing conditions. Subsequently, gel strips with separated α-chains were cut and submerged for 1 h in a protein-loading buffer supplemented with β-mercaptoethanol. Next, the gel strip was placed horizontally on the top of a new polyacrylamide gel and electrophoresis was carried out. Finally, protein bands were transferred to nitrocellulose membranes and the α1(II) chains were specifically detected by Western blot as described above.

Analysis of the conformational integrity of the R992C collagen II.

The thermostability of the R992C collagen was measured by brief protease digestion, as described [38]. In brief, the pepsin-treated samples dissolved in a 0.1 M Tris-HCl buffer (pH 7.4) supplemented with 0.4 M NaCl and 25 mM EDTA were pre-incubated for 30 min at selected temperatures and then treated for 3 min with a mixture of trypsin (100 µg/ml, Sigma-Aldrich) and chymotrypsin (250 µg/ml, Sigma-Aldrich). Enzymatic digestion was terminated by adding 0.1-volume of 5 mg/ml soybean trypsin inhibitor (Sigma-Aldrich). Protease-treated collagen samples were electrophoresed in reducing conditions in 7.5% polyacrylamide-SDS gels and then the protein bands were transferred to nitrocellulose membranes and analyzed by Western blot as described above. Relative amounts of the protease-resistant α1(II) chains in analyzed samples were determined by measuring the pixel intensities of the α1(II)-positive bands. Considering the relative value of the intensity of an α1(II) band derived from collagen digested at 30°C a 100%, the relative values of the intensities of α1(II) bands derived by enzymatic digestion at higher temperatures were measured. The mean values from three independent experiments were calculated and plotted against temperature (Sigma Plot v. 8.02, SPSS Inc.)

Computer modeling of the R992C mutation site.

A computer model of the triple-helical region spanning the R992C mutation site was generated by the Sybyl7.3 program (Tripos, Inc.) as described [18,39]. Molecular surfaces of the analyzed collagen fragments were generated using the MOLCAD module of the Sybyl program [20,40]. The same module was used to calculate electrostatic potential (EP, physical unit; kcal/mol.e) and the area of the analyzed surfaces [41].

Unconditional and Tet-regulated expression of Pro-GFP and Pro-GFP^{Tet} variants in SW-1353 cells.

The WT Pro-GFP and R992C Pro-GFP variants were unconditionally expressed in the chondrocytic SW-1353 cell line (ATCC; HTB-94), as described [22,23]. This cell line was also employed to express the WT Pro-GFP^{Tet} and R992C Pro-GFP^{Tet} variants in the Tet-dependent fashion, as described [23]. Selected SW-1353 clones stably expressing Pro-GFP or Pro-GFP^{Tet} variants were cultured in Dulbecco's Modified Eagle's Media (DMEM) supplemented with 10% fetal bovine serum (FBS) or Tet-system-certified FBS (Clontech Laboratories, Inc.) and 40 μg/ml of L-ascorbic acid phosphate magnesium salt (Wako, Japan). Expression of the Pro-GFP^{Tet} variants was initiated by culturing the Tet-responsive SW-1353 cells in the presence of 1 μg/ml of doxycycline (Clontech Laboratories, Inc.). Biosynthesis of Pro-GFP and Pro-GFP^{Tet} variants in selected SW-1353 clones was confirmed at the mRNA and protein levels, as described [22,23]. Moreover, the kinetics of secretion of analyzed Pro-GFP variants were studied, as described [22].

TUNEL and cleaved PARP assays.

Confluent cells expressing Pro-GFP and Pro-GFP^{Tet} variants were cultured for 12 days and then analyzed for the markers of apoptosis, as described [23]. In one set of experiments the presence of fragmented DNA was analyzed by TUNEL assays (Roche). In these analyses untransfected SW-1353 cells treated with 3 units/ml of DNaseI (Sigma-Aldrich) served as a positive control. The cells were observed under a fluorescence microscope (Eclipse E600; Nikon) equipped with appropriate filter sets and a monochromatic digital camera (CoolSnap CF; Photometrics, Inc.) controlled by Image-Pro AMS software (version 5.1.0.2.0, Media

Cybernetics, Inc). The total number of cells in viewing areas was determined by DAPI-positive nuclei. Subsequently, the percentage of TUNEL-DAPI-positive cells in analyzed groups was calculated [23].

In addition to the TUNEL assays, Western blot analyses of cleaved PARP were employed to identify apoptosis, as described [23]. In these assays cleaved PARP was detected with primary rabbit anti-cleaved PARP antibodies (Cell Signaling Technology, Inc.) and secondary anti-rabbit IgG conjugated to HRP (Sigma-Aldrich). Employing a gel imaging system (UVP, LLC), bands corresponding to the cleaved PARP were visualized by chemiluminescence. The same nitrocellulose membranes were also probed with monoclonal anti-glyceraldehyde-3-phosphate dehydrogenase (GAPDH) antibodies (Santa Cruz Biotechnology, Inc.). Relative amounts of cleaved PARP in analyzed samples were determined by measuring the pixel intensities of the cleaved PARP-positive bands. To correct densitometry data for any differences in loading the samples onto polyacrylamide gels, final calculations were done assuming equal content of GAPDH in all analyzed samples. The ratio of relative amount of cleaved PARP from cells expressing the R992C Pro-GFP to cleaved PARP from cells expressing WT Pro-GFP was calculated. In experiments with Pro-GFP^{Tet} variants, the ratio of relative amount of cleaved PARP from Dox-induced cells to that from corresponding non-induced cells was calculated. Statistical significances of differences between the calculated means were analyzed by the Student's *t* test (GraphPad Software, Inc.).

Measurements of selected indicators of ER stress.

It has been shown that some mutations in fibrillar collagens are associated with increased expression of chaperones such as BiP and PDI [2,3,23]. To specifically determine whether ER

stress-related changes in the relative amounts of these proteins were caused by the presence of the R992C mutant, we employed cells expressing R992C Pro-GFP and R992C Pro-GFP^{Tet} variants. The presence of intracellular BiP and PDI was analyzed by Western blot assays with rat monoclonal anti-BiP and goat anti-PDI antibodies (Santa Cruz Biotechnology, Inc), respectively. Consistent with other Western blot assays GAPDH-positive bands served as the internal control.

Analysis of LH and P4H.

Analysis of LH (EC 1.14.11.4) and P4H (EC 1.14.11.2) in lysates from cells expressing Pro-GFP variants was done by Western blot assays. Primary goat anti-LH antibodies (Santa Cruz Biotechnology, Inc.) and secondary donkey anti-goat IgG antibodies conjugated to horseradish peroxidase (HRP; Rockland Immunochemicals) were used to detect LH-specific bands. Primary rabbit antibodies against the α1 subunit of P4H and HRP-conjugated secondary anti-rabbit IgG were employed to detect the P4Hα-specific bands (Sigma-Aldrich). In these assays GAPDH served as internal control and was detected as described above.

Fluorescence microscopy assays of in situ colocalization of the R992C Pro-GFP with BiP, PDI, and P4H.

It has been shown that in response to the ER stress, BiP and PDI function as chaperones by binding to the misfolded mutant collagen molecules, thereby facilitating their intracellular retention. To determine the potential involvement of BiP and PDI in controlling intracellular retention and folding of the R992C collagen, we assayed the colocalization of these interacting partners. We also analyzed whether during ER stress PDI interacts with Pro-GFP variants independently or as the β-subunit of P4H. In these assays we studied colocalization of Pro-GFP

variants with the catalytical α-subunit of the P4H. In previous studies we analyzed possible Pro-GFP/BiP and Pro-GFP/PDI binding by co-immunoprecipitation assays [23]. Because the studied interactions are weak, these assays are complex and require employing a cross-linking compound that prevents dissociation of interactants in the detergent-rich environment of a cell lysis buffer. Thus, in this study intracellular colocalization of the R992C Pro-GFP with BiP, PDI, and P4Hα was assayed after immunostaining of these specific binding partners with rabbit anti-BiP (Santa Cruz Biotechnology, Inc.), rabbit anti-PDI (Santa Cruz Biotechnology, Inc.) or rabbit anti-P4Hα antibodies (Sigma-Aldrich), respectively. Specific secondary antibodies conjugated with Alexa Fluor 594 were employed to visualize intracellular localization of analyzed proteins (Invitrogen, Inc.). At first, the cells were permeabilized with 0.2% Tween 20 and then the samples were blocked with appropriate serum to minimize non-specific binding of antibodies. Subsequently, the samples were incubated with primary and then secondary antibodies at conditions optimized in pilot studies. Finally, nuclei were stained with DAPI and the samples were mounted with a mounting media reagent (Prolong Gold; Invitrogen, Inc.). To determine the extent of nonspecific immunostaining and the degree of autofluorescence, samples treated only with secondary antibodies and those with no antibody treatment were prepared as controls.

The immunostained cells were observed with a microscope (Eclipse E600, Nikon, Japan) equipped with a computer-controlled Z-stack stage and sets of chromophor-specific filters and the Plan Fluor 40x/1.3 Oil objective (Nikon, Japan). Images of the cells were acquired with a monochromatic digital camera (CoolSnap CF; Photometrics, Inc.) controlled by Image-Pro AMS software (version 5.1.0.2.0, Media Cybernetics, Inc). Control samples were employed to correct for the background fluorescence. Pairs of images taken with filters specific for GFP and Alexa Fluor 594 were pseudo-colored and then merged. Following deconvolution, colocalization of

pixels from green and red channels was measured by using the "Colocalization Module" of the Image-Pro AMS software. Colocalization of pixels from a cytoplasm region of analyzed cells was expressed as the overlap coefficient (*R*). This parameter, defined by Manders *et al*., represents a true degree of colocalization of defined pixels and is not sensitive to the limitations of typical fluorescence imaging, such as efficiency of hybridization, sample photobleaching, and camera quantum efficiency [42].

Acknowledgements

This work was supported by the National Health Institutes to A.F. (5R01AR049537-06).

References

1. Prockop, D. J. & Kivirikko, K. I. (1995). Collagens: molecular biology, diseases, and potentials for therapy. *Annu Rev Biochem* **64**, 403-434.
2. Chessler, S. D. & Byers, P. H. (1992). Defective folding and stable association with protein disulfide isomerase/prolyl hydroxylase of type I procollagen with a deletion in the pro alpha 2(I) chain that preserves the Gly-X-Y repeat pattern. *J Biol Chem* **267**, 7751-7757.
3. Chessler, S. D. & Byers, P. H. (1993). BiP binds type I procollagen pro alpha chains with mutations in the carboxyl-terminal propeptide synthesized by cells from patients with osteogenesis imperfecta. *J Biol Chem* **268**, 18226-18233.

4. McLaughlin, S. H. & Bulleid, N. J. (1998). Molecular recognition in procollagen chain assembly. *Matrix Biol* **16**, 369-377.

5. Tasab, M., Batten, M. R. & Bulleid, N. J. (2000). Hsp47: a molecular chaperone that interacts with and stabilizes correctly-folded procollagen. *Embo J* **19**, 2204-2211.

6. Walmsley, A. R., Batten, M. R., Lad, U. & Bulleid, N. J. (1999). Intracellular retention of procollagen within the endoplasmic reticulum is mediated by prolyl 4-hydroxylase. *J Biol Chem* **274**, 14884-14892.

7. Olsen, B. R. (1995). Mutations in collagen genes resulting in metaphyseal and epiphyseal dysplasias. *Bone* **17**, 45S-49S.

8. Kuivaniemi, H., Tromp, G. & Prockop, D. J. (1991). Mutations in collagen genes: causes of rare and some common diseases in humans. *Faseb J* **5**, 2052-2060.

9. Bleasel, J. F., Bisagni-Faure, A., Holderbaum, D., Vacher-Lavenu, M. C., Haqqi, T. M., Moskowitz, R. W. & Menkes, C. J. (1995). Type II procollagen gene (COL2A1) mutation in exon 11 associated with spondyloepiphyseal dysplasia, tall stature and precocious osteoarthritis. *J Rheumatol* **22**, 255-261.

10. Bleasel, J. F., Holderbaum, D., Mallock, V., Haqqi, T. M., Williams, H. J. & Moskowitz, R. W. (1996). Hereditary osteoarthritis with mild spondyloepiphyseal dysplasia--are there "hot spots" on COL2A1? *J Rheumatol* **23**, 1594-1598.

11. Bleasel, J. F., Holderbaum, D., Brancolini, V., Moskowitz, R. W., Haqqi, T. M., Considine, E., Prockop, D. J., Devoto, M. & Williams, C. J. (1996). Arg519-Cys mutation in COL2A1: evidence for multiple founders. *Ann N Y Acad Sci* **785**, 215-218.

12. Knowlton, R. G., Katzenstein, P. L., Moskowitz, R. W., Weaver, E. J., Malemud, C. J., Pathria, M. N., Jimenez, S. A. & Prockop, D. J. (1990). Genetic linkage of a

polymorphism in the type II procollagen gene (COL2A1) to primary osteoarthritis associated with mild chondrodysplasia. *N Engl J Med* **322**, 526-530.

13. Hoornaert, K. P., Dewinter, C., Vereecke, I., Beemer, F. A., Courtens, W., Fryer, A., Fryssira, H., Lees, M., Mullner-Eidenbock, A., Rimoin, D. L., Siderius, L., Superti-Furga, A., Temple, K., Willems, P. J., Zankl, A., Zweier, C., De Paepe, A., Coucke, P. & Mortier, G. R. (2006). The phenotypic spectrum in patients with arginine to cysteine mutations in the COL2A1 gene. *J Med Genet* **43**, 406-413.

14. Williams, C. J., Considine, E. L., Knowlton, R. G., Reginato, A., Neumann, G., Harrison, D., Buxton, P., Jimenez, S. & Prockop, D. J. (1993). Spondyloepiphyseal dysplasia and precocious osteoarthritis in a family with an Arg75-->Cys mutation in the procollagen type II gene (COL2A1). *Hum Genet* **92**, 499-505.

15. Chan, D., Taylor, T. K. & Cole, W. G. (1993). Characterization of an arginine 789 to cysteine substitution in alpha 1 (II) collagen chains of a patient with spondyloepiphyseal dysplasia. *J Biol Chem* **268**, 15238-15245.

16. Ballo, R., Beighton, P. H. & Ramesar, R. S. (1998). Stickler-like syndrome due to a dominant negative mutation in the COL2A1 gene. *Am J Med Genet* **80**, 6-11.

17. Richards, A. J., Baguley, D. M., Yates, J. R., Lane, C., Nicol, M., Harper, P. S., Scott, J. D. & Snead, M. P. (2000). Variation in the vitreous phenotype of Stickler syndrome can be caused by different amino acid substitutions in the X position of the type II collagen Gly-X-Y triple helix. *Am J Hum Genet* **67**, 1083-1094.

18. Fertala, A., Ala-Kokko, L., Wiaderkiewicz, R. & Prockop, D. J. (1997). Collagen II containing a Cys substitution for arg-alpha1-519. Homotrimeric monomers containing the

mutation do not assemble into fibrils but alter the self-assembly of the normal protein. *J Biol Chem* **272**, 6457-6464.

19. Fertala, A., Sieron, A. L., Adachi, E. & Jimenez, S. A. (2001). Collagen II containing a Cys substitution for Arg-alpha1-519: abnormal interactions of the mutated molecules with collagen IX. *Biochemistry* **40**, 14422-14428.

20. Steplewski, A., Brittingham, R., Jimenez, S. A. & Fertala, A. (2005). Single amino acid substitutions in the C-terminus of collagen II alter its affinity for collagen IX. *Biochem Biophys Res Commun* **335**, 749-755.

21. Steplewski, A., Ito, H., Rucker, E., Brittingham, R. J., Alabyeva, T., Gandhi, M., Ko, F. K., Birk, D. E., Jimenez, S. A. & Fertala, A. (2004). Position of single amino acid substitutions in the collagen triple helix determines their effect on structure of collagen fibrils. *J Struct Biol* **148**, 326-337.

22. Ito, H., Rucker, E., Steplewski, A., McAdams, E., Brittingham, R. J., Alabyeva, T. & Fertala, A. (2005). Guilty by association: some collagen II mutants alter the formation of ECM as a result of atypical interaction with fibronectin. *J Mol Biol* **352**, 382-395.

23. Hintze, V., Steplewski, A., Ito, H., Jensen, D. A., Rodeck, U. & Fertala, A. (2008). Cells expressing partially unfolded R789C/p.R989C type II procollagen mutant associated with spondyloepiphyseal dysplasia undergo apoptosis. *Hum Mutat* **29**, 841-851.

24. Donahue, L. R., Chang, B., Mohan, S., Miyakoshi, N., Wergedal, J. E., Baylink, D. J., Hawes, N. L., Rosen, C. J., Ward-Bailey, P., Zheng, Q. Y., Bronson, R. T., Johnson, K. R. & Davisson, M. T. (2003). A missense mutation in the mouse Col2a1 gene causes spondyloepiphyseal dysplasia congenita, hearing loss, and retinoschisis. *J Bone Miner Res* **18**, 1612-1621.

25. Fertala, A., Sieron, A. L., Ganguly, A., Li, S. W., Ala-Kokko, L., Anumula, K. R. & Prockop, D. J. (1994). Synthesis of recombinant human procollagen II in a stably transfected tumour cell line (HT1080). *Biochem J* **298**, 31-37.

26. Gossen, M., Freundlieb, S., Bender, G., Muller, G., Hillen, W. & Bujard, H. (1995). Transcriptional activation by tetracyclines in mammalian cells. *Science* **268**, 1766-1769.

27. Forlino, A., Keene, D. R., Schmidt, K. & Marini, J. C. (1998). An alpha2(I) glycine to aspartate substitution is responsible for the presence of a kink in type I collagen in a lethal case of osteogenesis imperfecta. *Matrix Biol* **17**, 575-584.

28. Steplewski, A., Majsterek, I., McAdams, E., Rucker, E., Brittingham, R. J., Ito, H., Hirai, K., Adachi, E., Jimenez, S. A. & Fertala, A. (2004). Thermostability gradient in the collagen triple helix reveals its multi-domain structure. *J Mol Biol* **338**, 989-998.

29. Eyre, D. R., Weis, M. A. & Moskowitz, R. W. (1991). Cartilage expression of a type II collagen mutation in an inherited form of osteoarthritis associated with a mild chondrodysplasia. *J Clin Invest* **87**, 357-361.

30. Privalov, P. L. (1982). Stability of proteins. Proteins which do not present a single cooperative system. *Adv Protein Chem* **35**, 1-104.

31. Westerhausen, A., Kishi, J. & Prockop, D. J. (1990). Mutations that substitute serine for glycine alpha 1-598 and glycine alpha 1-631 in type I procollagen. The effects on thermal unfolding of the triple helix are position-specific and demonstrate that the protein unfolds through a series of cooperative blocks. *J Biol Chem* **265**, 13995-14000.

32. Persikov, A. V., Ramshaw, J. A., Kirkpatrick, A. & Brodsky, B. (2000). Amino acid propensities for the collagen triple-helix. *Biochemistry* **39**, 14960-14967.

33. Arnold, W. V., Fertala, A., Sieron, A. L., Hattori, H., Mechling, D., Bachinger, H. P. & Prockop, D. J. (1998). Recombinant procollagen II: Deletion of D period segments identifies sequences that are required for helix stabilization and generates a temperature-sensitive N-proteinase cleavage site. *J Biol Chem* **273**, 31822-31828.

34. Bassuk, J. A. & Berg, R. A. (1989). Protein disulphide isomerase, a multifunctional endoplasmic reticulum protein. *Matrix* **9**, 244-258.

35. Gething, M. J. & Sambrook, J. (1992). Protein folding in the cell. *Nature* **355**, 33-45.

36. Arnold, W. V., Sieron, A. L., Fertala, A., Bachinger, H. P., Mechling, D. & Prockop, D. J. (1997). A cDNA cassette system for the synthesis of recombinant procollagens. Variants of procollagen II lacking a D-period are secreted as triple- helical monomers. *Matrix Biol* **16**, 105-116.

37. Majsterek, I., McAdams, E., Adachi, E., Dhume, S. T. & Fertala, A. (2003). Prospects and limitations of the rational engineering of fibrillar collagens. *Protein Sci* **12**, 2063-2072.

38. Sieron, A. L., Fertala, A., Ala-Kokko, L. & Prockop, D. J. (1993). Deletion of a large domain in recombinant human procollagen II does not alter the thermal stability of the triple helix. *J Biol Chem* **268**, 21232-21237.

39. Chen, J. M., Sheldon, A. & Pincus, M. R. (1995). Three-dimensional energy-minimized model of human type II "Smith" collagen microfibril. *J Biomol Struct Dyn* **12**, 1129-1159.

40. Connolly, M. L. (1983). Solvent-accessible surfaces of proteins and nucleic acids. *Science* **221**, 709-713.

41. Warwicker, J. & Watson, H. C. (1982). Calculation of the electric potential in the active site cleft due to alpha-helix dipoles. *J Mol Biol* **157**, 671-679.

42. Manders, E. M. M., Verbbk, F. J. & Aten, J. A. (1993). Measurement of co-localization of objects in dual-color confocal images. *J Microsc* **169**, 375-382.

FIGURE LEGENDS

Figure 1. Analysis of intact and processed R992C Pro-GFP.

A: Western blot assays of WT Pro-GFP and R992C Pro-GFP variants freshly isolated from cell culture media and electrophoresed in 6% polyacrylamide gels. B: Analysis of pepsin-processed collagen II variants after their treatment with glycosidases. Note that after electrophoresis in a 7.5% gel only a relatively small shift in migration was seen after glycosidase treatment. Symbols: WT Pro-GFP and WT, wild type procollagen II and collagen II, respectively; R992C Pro-GFP and R992C, procollagen II and collagen II mutant harboring R992C substitution, respectively; Pro-α1-GFP, GFP-tagged procollagen chains; α1, pepsin-treated collagen chains; +/- indicates the presence or the absence of glycosidases (Glyc) in analyzed samples; asterisks in panel B indicate partially degraded mutant collagen. Positions of molecular mass markers and types of antibodies employed in detecting procollagens and collagens are also indicated.

Figure 2. Analysis of disulfide bonds formed between α1 chains of the R992C mutant.

A: Analysis of the WT collagen variant. B: Analysis of disulfide-linked α1 chains present in the R992C collagen II. Collagen II was separated in non-reducing conditions in a 7.5%

polyacrylamide gel (left panel). Next, a gel strip with separated collagen chains was cut and submerged in the reducing agent. Subsequently, the gel strip was placed at the top of another 7.5% gel. After electrophoresis, collagen bands were detected with anti-collagen II antibodies. Symbols: WT, wild type collagen II; R992C collagen II mutant harboring R992C substitution; α1 and $^{S\text{-}S}$α1, single collagen chains and disulfide-linked chains; (+/-) β indicates the presence or the absence of β-mercaptoethanol in analyzed samples; arrows in panel B indicate direction of electrophoretic migration of analyzed collagen.

Figure 3. Assays of the thermostability of the R992C mutant.

Followed preincubation at increasing temperatures, collagen II samples were subjected to brief proteinase digestion. The digested samples were electrophoresed in 7.5% polyacrylamide gels in reducing conditions and then α1(II) chains were visualized by Western blot (A). Subsequently, the relative pixel intensities of α1(II) chains were measured by densitometry. A graphic representation of changes in the relative amount of triple-helical collagen II in response to increasing temperature is shown in the panel B. Symbols: WT, wild type collagen II; R992C, collagen II mutant harboring R992C substitution; α1, α1(II) chains; α1 Int, intermediate products of enzymatic cleavage of the α1(II) chains; closed circles represent WT while open circles represent the R992C mutant.

Figure 4. A computer model of the region encompassing the R992C mutation site.

Surfaces representing electron densities were generated using a computer program. The left panel illustrates the electrostatic potentials (EP) of regions encompassing R992 and C992 sites. The right panel is a front view at the mutation site (indicated by a plane in the left panel).

Relatively large surface with the EP values similar to those of the R992 site present in the WT collagen is significantly reduced in the R992C mutant. The intramolecular disulfide bond formed between C992 residues is indicated with two asterisks while the free C992 residue is indicated with one asterisk. R990 and E995 residues neighboring the mutation site are indicated for reference. Legend: Color code used to indicate differences in the EP: red, highly positive EP; blue, highly negative EP.

Figure 5. Constant production of the Pro-GFP variants and Dox-dependent production of Pro-GFP^{Tet} variants by SW-1353 cells.

A: RT-PCR assays of Pro-GFP expression and Dox-dependent expression of Pro-GFP^{Tet} variants. In all samples, analyses of GAPDH were employed as controls. B: Western blot analysis of Pro-GFP and Pro-GFP^{Tet} variants extracted from cells cultured in the absence (-) or presence (+) of Dox. Note: All procollagen II-GFP chimeras were detected with anti-GFP antibody. In the same samples GAPDH was detected with anti-GAPDH antibody. Symbols: WT, samples that include wild type procollagen II; R992C, samples that include R992C collagen II; Pro-GFP, cells that unconditionally express procollagen II-GFP chimeras; Pro-GFP^{Tet}, cells that express procollagen II-GFP chimera whose expression is Tet-dependent; Dox +/- indicates the presence or absence of Dox in cell culture media.

Figure 6. Kinetics of secretion of procollagen II variants from SW-1353 cells.

A: Western blot assays of secretion of Pro-GFP variants with anti-GFP antibody. B: Graphic representation of rates of secretion of analyzed Pro-GFP variants. Mean values of the relative intensities of protein bands were derived from three independent measurements. For the R992C

Pro-GFP, data from two different clones were included. For both, the WT and R992C variants the pixel intensity values at the indicated time points were calculated as a percent of the value for the WT Pro-GFP measured at the 6^{th} hour. Note that the intensity of WT Pro-GFP at 6^{th} hour is considered 100%. Symbols: WT, samples that include wild type collagen; R992C, samples that include R992C mutants.

Figure 7. TUNEL assays of apoptosis in cells expressing type II collagen mutants.

A: A representative image of nuclei of cells analyzed by TUNEL. DAPI-stained nuclei (left), TUNEL-positive nucleus (center) and merged images of both (right) are presented.

B: A graphic representation of apoptotic indexes in cells expressing the Pro-GFP variants and the Pro-GFP^{Tet} variants cultured in the absence (-) or presence (+) of Dox. The apoptotic index is defined as the percentage of TUNEL-positive nuclei out of the total number of DAPI-positive nuclei. Note: Quantitative results for the R992C mutant are based on measurements of two independent clones. Symbols: WT, cells that express wild type collagen II; R992C, the R992C collagen II mutant; Dox (+/-), the presence or absence of Dox in cell culture media.

Figure 8. Assays of cleaved PARP in cells expressing Pro-GFP and Pro-GFP^{Tet} variants.

A: Western blot assays of cleaved PARP in cells expressing Pro-GFP and Pro-GFP^{Tet} variants.

B: Analysis of relative amounts of cleaved PARP in cells expressing Pro-GFP variants and Pro-GFP^{Tet} variants. On the left, the ratio of the cleaved PARP present in cells expressing the R992C Pro-GFP mutant to the cleaved PARP in cells expressing the WT Pro-GFP variant is presented. Mean values and standard errors of means (in parentheses) are presented. Statistical significances of differences between means and the number of independent measurements are also indicated.

On the right, analyses of the relative amounts of cleaved PARP in cells expressing Pro-GFP^{Tet} variants before (-) and after (+) Dox induction. The changes were calculated as ratios of cleaved PARP present in induced and non-induced cells. Mean values and standard errors of means (in parentheses) are presented. Statistical significances of differences between means and the number of independent measurements are also indicated. Note: Quantitative results for the R992C mutant are based on measurements of two independent clones. Symbols: WT, cells that express wild type collagen II; R992C, samples that include the R992C collagen II mutant; Pro-GFP, cells that unconditionally express the respective collagen II variant; Pro-GFP^{Tet}, cells that express the respective collagen II variant in the Tet-dependent fashion; Dox (+/-), the presence or absence of Dox in cell culture media; cPARP, cleaved PARP; GAPDH, GAPDH-positive bands.

Figure 9. Assays of chaperones in cells expressing Pro-GFP and Pro-GFP^{Tet} variants.

A and B: Assays of PDI in cells expressing Pro-GFP and Pro-GFP^{Tet} variants. C and D: Assays of BiP in cells expressing Pro-GFP and Pro-GFP^{Tet} variants. E and F: Assays of LH in cells expressing Pro-GFP and Pro-GFP^{Tet} variants. In each graph, the ratios of chaperones present in cells expressing Pro-GFP mutants to chaperones in cells expressing WT Pro-GFP are presented. Mean values and standard errors of means (in parentheses) are presented. Statistical significance of differences between means and the number of independent measurements are also indicated. Moreover, in each graphic panel analyses of the relative amounts of chaperones in cells expressing Pro-GFP^{Tet} variants before (-) and after (+) Dox induction are presented. The changes were calculated as ratios of chaperones present in induced and non-induced cells. Mean values and standard errors of means (in parentheses) are presented. Statistical significance of differences between means and the number of independent measurements are also indicated.

Note: Quantitative results for the R992C mutant are based on measurements of two independent clones. Symbols: WT, cells that express the wild type collagen II; R992C, samples that include the R992C mutant; Pro-GFP, cells that unconditionally express the respective collagen II variant; Pro-GFP^{Tet}, cells that express the respective collagen II variant in the Tet-dependent fashion; Dox (+/-), the presence or absence of Dox in cell culture media; LH, Lysyl hydroxylase-positive bands; GAPDH, GAPDH-positive bands.

Figure 10. Colocalization of Pro-GFP with BiP, PDI, and P4H.

Representative images of cells expressing the R992C Pro-GFP and immunostained for BiP, PDI or P4H are presented. Red channels, green channels and mergers of both together with DAPI-stained nuclei are depicted.

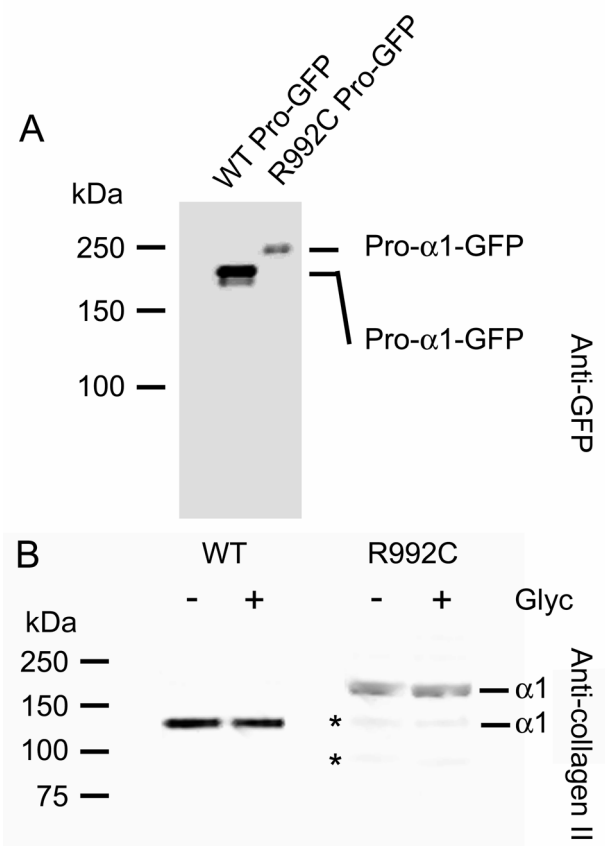
A
WT Pro-GFP
R992C Pro-GFP
kDa
250
150
100
Pro-α1-GFP
Pro-α1-GFP
Anti-GFP
B
WT
R992C
- + - +
Glyc
kDa
250
150
100
75
α1
α1
*
*
Anti-collagen II

Figure 1

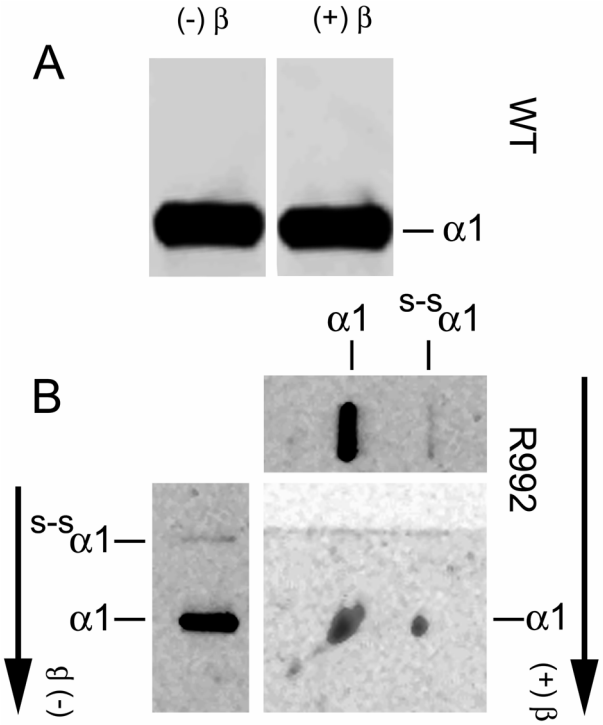

Figure 2

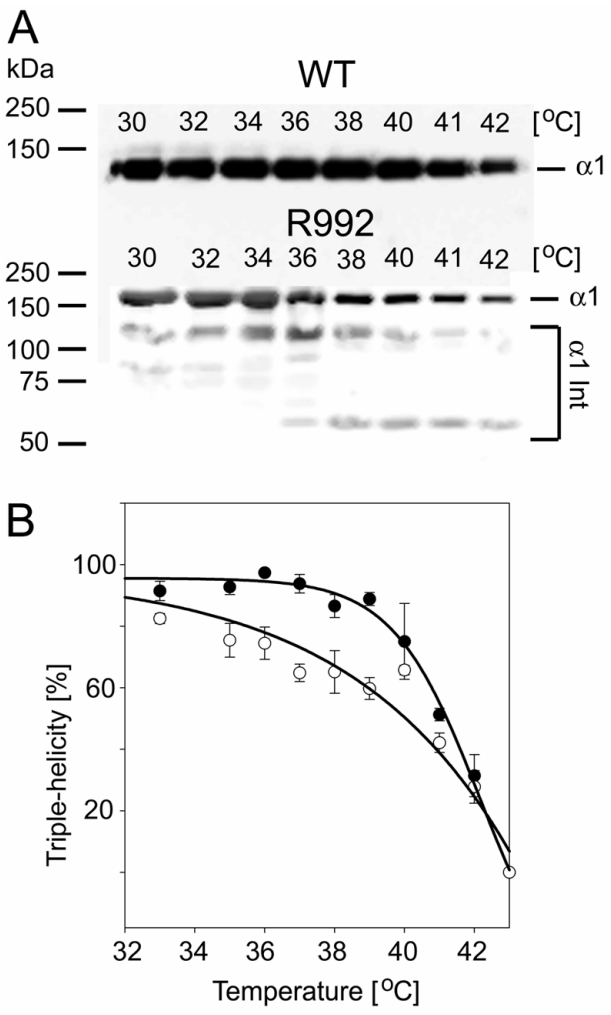
A
kDa
WT
250
150
30 32 34 36 38 40 41 42 [°C]
α1
R992
30 32 34 36 38 40 41 42 [°C]
250
150
100
75
50
α1
α1 Int
B
100
60
20
Triple-helicity [%]
32 34 36 38 40 42
Temperature [°C]

Figure 3

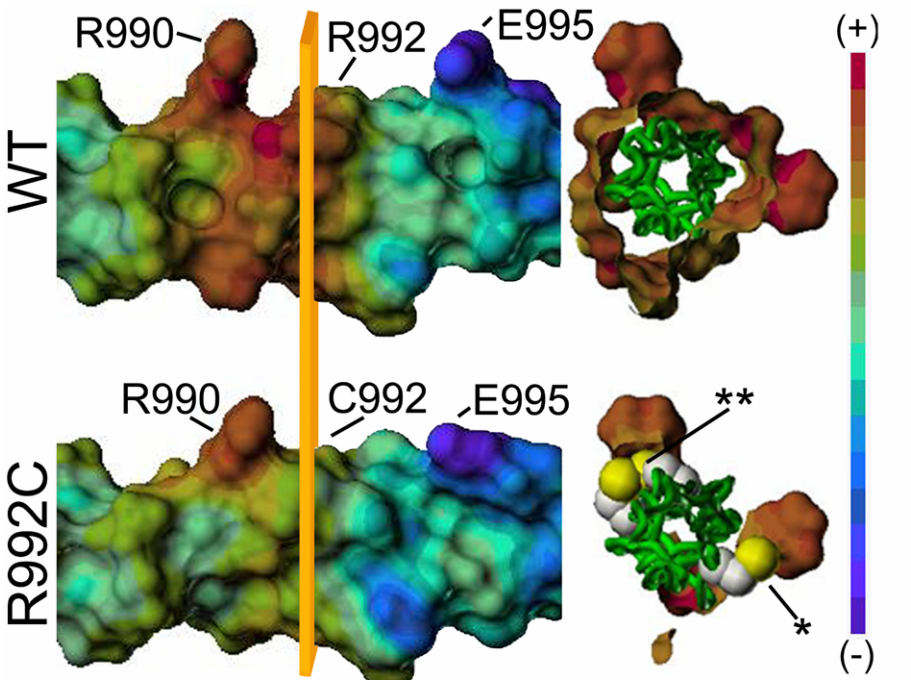

Figure 4

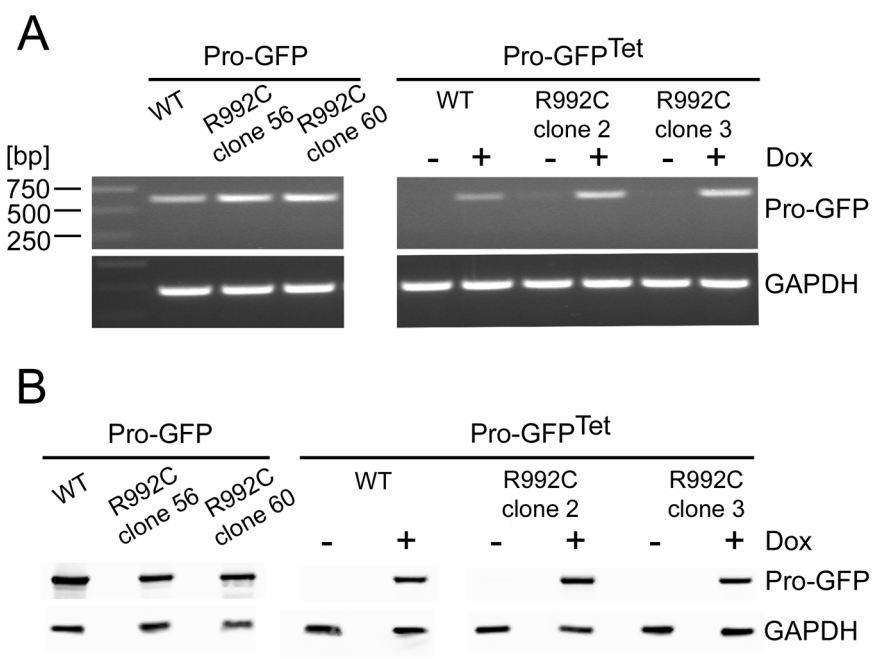
A
Pro-GFP
Pro-GFP^Tet
WT
R992C clone 56
R992C clone 60
WT
R992C clone 2
R992C clone 3
[bp]
750
500
250
- + - + - + Dox
Pro-GFP
GAPDH
B
Pro-GFP
Pro-GFP^Tet
WT
R992C clone 56
R992C clone 60
WT
R992C clone 2
R992C clone 3
- + - + - + Dox
Pro-GFP
GAPDH

Figure 5

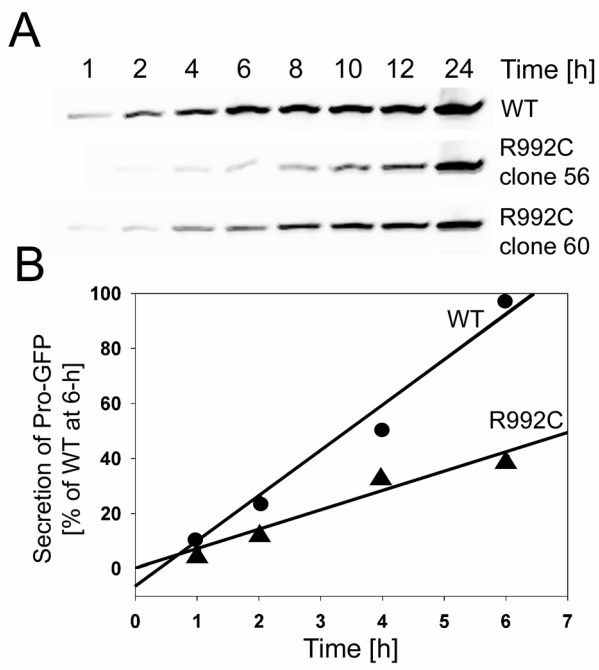
A
1
2
4
6
8
10
12
24
Time [h]
WT
R992C
clone 56
R992C
clone 60
B
Secretion of Pro-GFP
[% of WT at 6-h]
100
80
60
40
20
0
WT
R992C
0
1
2
3
4
5
6
7
Time [h]

Figure 6

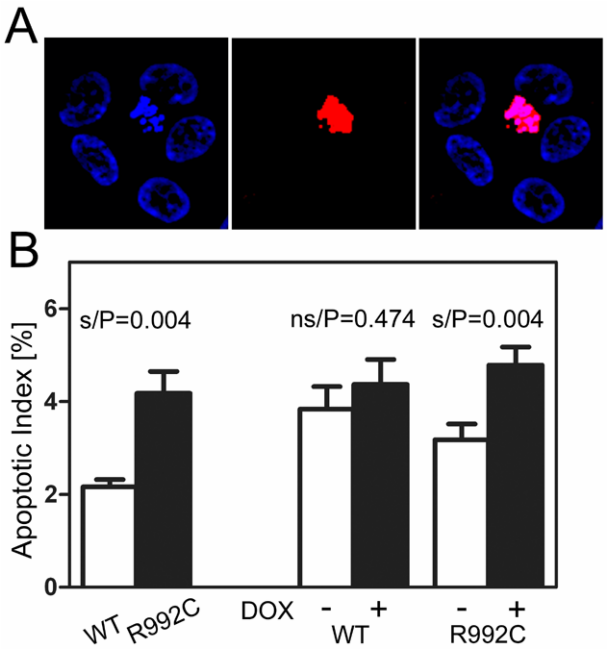
A
B
Apoptotic Index [%]
0
2
4
6
s/P=0.004
ns/P=0.474
s/P=0.004
WT
R992C
DOX
-
+
WT
-
+
R992C

Figure 7

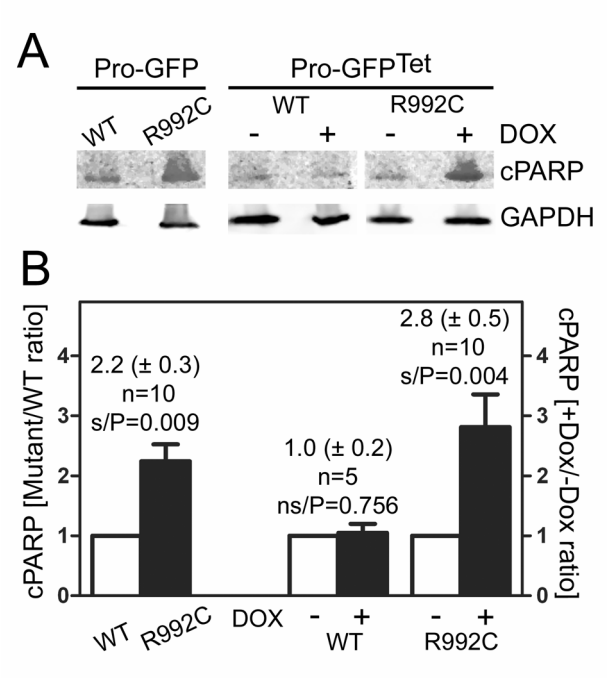
A
Pro-GFP
Pro-GFPTet
WT
R992C
WT
R992C
- + - + DOX
cPARP
GAPDH
B
cPARP [Mutant/WT ratio]
cPARP [+Dox/-Dox ratio]
2.2 (± 0.3)
n=10
s/P=0.009
1.0 (± 0.2)
n=5
ns/P=0.756
2.8 (± 0.5)
n=10
s/P=0.004
0
1
2
3
4
WT R992C DOX - + WT - + R992C

Figure 8

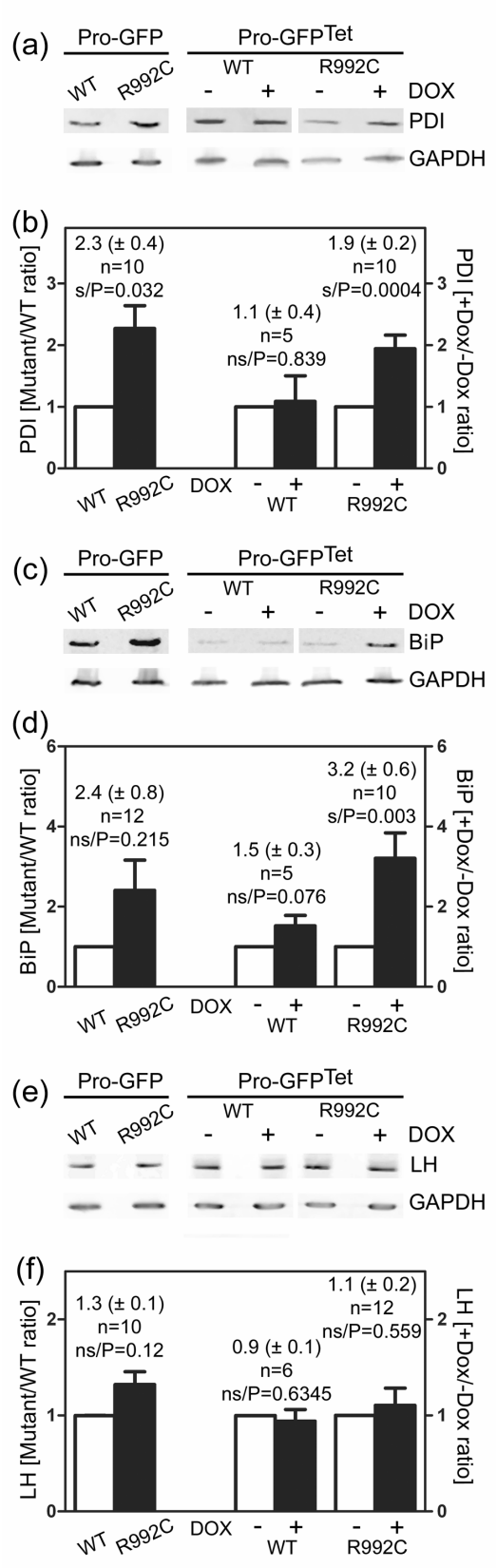
(a)
Pro-GFP
Pro-GFPTet
WT
R992C
WT
R992C
- + - + DOX
PDI
GAPDH
(b)
2.3 (± 0.4)
n=10
s/P=0.032
1.1 (± 0.4)
n=5
ns/P=0.839
1.9 (± 0.2)
n=10
s/P=0.0004
PDI [Mutant/WT ratio]
PDI [+Dox/-Dox ratio]
WT R992C DOX - + WT - + R992C
(c)
Pro-GFP
Pro-GFPTet
WT
R992C
WT
R992C
- + - + DOX
BiP
GAPDH
(d)
2.4 (± 0.8)
n=12
ns/P=0.215
1.5 (± 0.3)
n=5
ns/P=0.076
3.2 (± 0.6)
n=10
s/P=0.003
BiP [Mutant/WT ratio]
BiP [+Dox/-Dox ratio]
WT R992C DOX - + WT - + R992C
(e)
Pro-GFP
Pro-GFPTet
WT
R992C
WT
R992C
- + - + DOX
LH
GAPDH
(f)
1.3 (± 0.1)
n=10
ns/P=0.12
0.9 (± 0.1)
n=6
ns/P=0.6345
1.1 (± 0.2)
n=12
ns/P=0.559
LH [Mutant/WT ratio]
LH [+Dox/-Dox ratio]
WT R992C DOX - + WT - + R992C

Figure 9

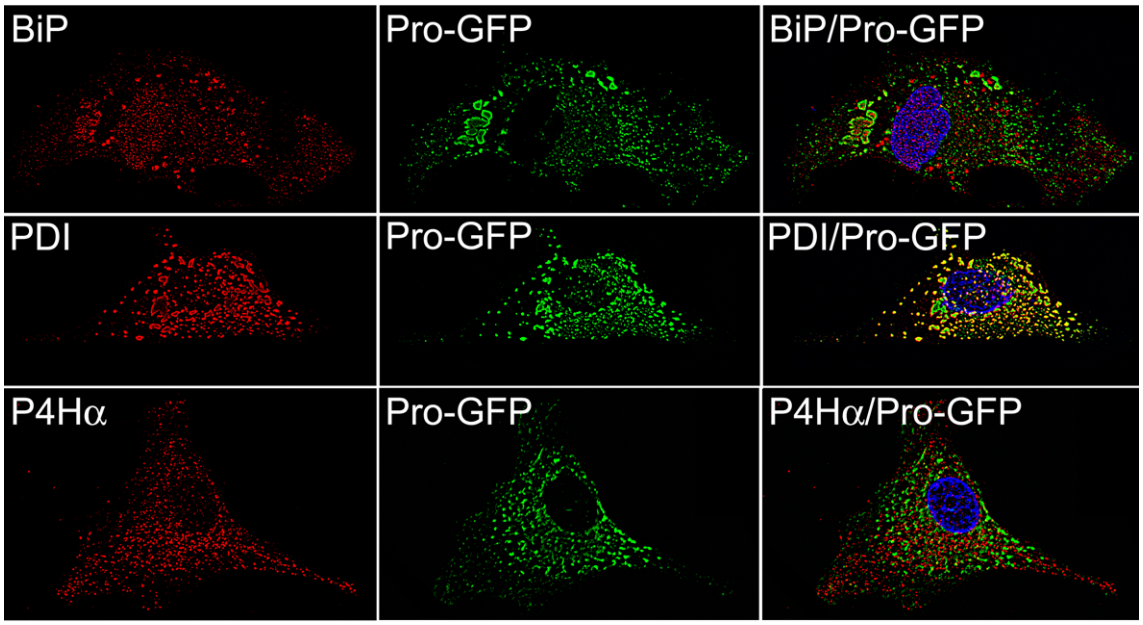
BiP
Pro-GFP
BiP/Pro-GFP
PDI
Pro-GFP
PDI/Pro-GFP
P4Hα
Pro-GFP
P4Hα/Pro-GFP

Figure 10